A Novel Compact High-Power X-Band Relativistic Magnetron With Diffraction Output

Ya. E. Krasik, J. G. Leopold, O. Belozerov, Y. P. Bliokh, E. Magid, G. Goldstein, and E. Schamiloglu

***Abstract*—In a recent publication [IEEE Trans. Plasma Sci. vol. 53, no. 11, pp. 3285–95, Nov. 2025], we reported on the operation of a novel X-band relativistic diffraction output magnetron (MDO) producing over 100 MW microwave power at ~9.7 GHz with ~50% maximum electronic efficiency. Here, we present the results of the performance of an MDO with a significantly shorter diffraction output antenna (DOA), which makes the overall dimensions smaller by half. Guided by 3-D particle-in-cell (PIC) simulations, the experiments demonstrate that this MDO produces ~9.5 GHz high-power microwave (HPM) pulses reaching ~120 MW maximum power, ≤ 20 ns pulse duration, and maximum instantaneous electronic efficiency reaching ~100%. We also demonstrated that this relativistic magnetron (RM) operates well when four longitudinal slits were cut symmetrically in the vanes of the eight-cavity anode block, transforming it into a four azimuthally segmented MDO. This allows one to decrease drastically the duration requirements of the external magnetic field and, respectively, the energy stored in the magnetic field's pulsed power supply. Finally, we present a novel design of a quarter-wave plate (QWP), which operates without breakdown at HPM powers exceeding 100 MW.**

***Index Terms*—High-power microwave (HPM), relativistic magnetrons (RMs), X-band.**

I. Introduction

RENEWED interest in high-power microwave (HPM) sources operating in the X-band[1] resulted in recent follow-up studies[2-4] of the first study by Kovalev, Fuks, (KF), and others in 1997[5] on an X-band relativistic magnetron (RM) in the diffraction output configuration (MDO). I n t his early publication, the RM consisted of an 8-cavity (A8) anode and operated with an explosive emission cathode, and microwaves were axially radiated through a diffraction output antenna (DOA). This MDO generated ~500 MW of microwave power at ~9 GHz with ≤ 15% efficiency and pulse duration ≤ 20 ns when it was powered by a ~500 kV, ~11 kA, and ~100 ns duration pulse.

The first experimental attempts to reproduce the operation of the KF MDO with a slightly modified DOA resulted in ~20 MW power, duration ≤ 50 ns, and a few percent efficiency of HPM generation when it was supplied by pulses of ≤300 kV, ≤ 3 kA, and pulse duration of ≤ 200 ns.[5] Next, based on the results of 3-D particle-in-cell (PIC) simulations,[2] the dimensions of the anode and DOA were changed significantly. Experimental research confirmed that this MDO generates HPM with over 100 MW power and with an electronic efficiency reaching 50%. However, the main disadvantage of this RM is its relatively large dimensions and requirements of a pulsed magnetic field in the range 0.5–0.7 T with a rise time of ~7.5 ms. The latter is necessary for allowing sufficient time for magnetic field diffusion through the anode block and the DOA, which dictates several kilojoules stored energy in the pulsed power source for generating the required pulsed magnetic field.

In this article, we present results of the operation of the RM with a significantly shorter DOA, which makes the overall dimensions of the MDO smaller by half. We demonstrate that this RM produces 9.5 GHz HPM with a power reaching ~120 MW, a pulse duration of ~20 ns, and an instantaneous electronic efficiency reaching ~100%. We also demonstrate that this RM operates well when four longitudinal slits were cut azimuthally in the center of four nonadjacent vanes of the 8-cavity anode block. This allows for much faster magnetic field penetration, resulting in a drastic decrease in the required duration of the external magnetic field, and consequently, in the energy stored in the magnetic field power supply, and it also makes repetitive operation possible.

II. Results of 3-D PIC Simulations of the Reduced Dimensions DOA

Extensive MAGIC PIC[7] simulations were performed in [2] to design and optimize the performance of a novel X-band MDO. The DOA of the resultant MDO extended to a relatively large inner diameter (105 mm), and its length was 200 mm. In the present simulations, the cathode was set to 8 mm diameter, the anode block was 21 mm long with 20 mm inner diameter, and with eight 5 mm deep resonant cavities of 20° azimuthal

This work was supported in part by Technion under Grant 2071448, in part by the Office of Naval Research Global (ONRG) under Grant N629092412093, and in part by the Office of Naval Research (ONR) through The University of New Mexico under Grant N00014-23-1-2072. The review of this article was arranged by Senior Editor X. Lu. *(Corresponding author: J. G. Leopold.)*

Ya. E. Krasik, J. G. Leopold, Y. P. Bliokh, E. Magid, and G. Goldstein are with the Physics Department, Technion, Haifa 3200003, Israel (e-mail: fnkrasik@physics.technion.ac.il; leopoldjg@physics.technion.ac.il; bliokh@physics.technion.ac.il; elhanan.magid@gmail.com; ga1g@walla.co.il).

O. Belozerov was with the Physics Department, Technion, Haifa 3200003, Israel. He is now with the Institute for Pulsed Power and Microwave Technology, KIT, 76139 Karlsruhe, Germany (e-mail: oleg.belozerov@kit.edu).

E. Schamiloglu is with the Department of Electrical and Computer Engineering, The University of New Mexico, Albuquerque, NM 87131 USA (e-mail: edls@unm.edu).

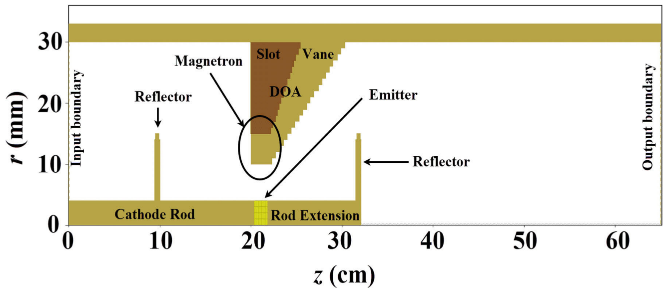

Fig. 1. Geometry of the simulated MDO. Here, the cross sections along the azimuthal center of one of the magnetron vanes (beige anode) and at the azimuthal center of one of the cavities (brown anode) are overdrawn.

width. To test a more compact design (see Fig. 1), we reduced the outer diameter of the DOA to 60 mm and changed slightly the inclination angles of the DOA conical extensions compared to those in [2], so that the conical slot extension extended 36 mm while the vane extended 89 mm along the outer waveguide's inner wall. These numerical simulations do not consider the existence of the plasma formed at the surface of the emitter, which can decrease the effective anode–cathode (A–K) gap, which here is only 6 mm.

In Fig. 2, the dependence of the input and output power calculated at the input and output boundaries, respectively (See Fig. 1), is drawn for different values of the applied axial magnetic fields [Fig. 1(a)–(d)]. Power is calculated as the Poynting flux through the boundary area perpendicular to the direction of the power flow. The voltage at the input boundary was set to 170 kV rising in 1 ns.

In the simulations, microwave generation begins only at magnetic fields $B_z \geq 0.4$ T. At $B_z = 0.4$ T [Fig. 2(a)], the maximum microwave power reaches ~150 MW at frequency $f \sim 9$ GHz. Low frequency (~250 MHz) HPM modulations appear at 0.45 T with maximum power slightly exceeding the input power [Fig. 1(b)] with the same $f \sim 9$ GHz. This behavior continues up to 0.55 T when at the low-frequency power modulations reach ~1.6 of the input power [Fig. 2(c)]. In the range of $B_z = 0.4$–0.55 T, the magnetron operates in the π-mode, which becomes a TE41 waveguide mode at the output boundary just as reported in [2]. At $B_z = 0.6$ T [Fig. 2(d)], there are still modulations with maximum power above the input power, which decay to a fixed power of ~75 MW. There is, though, a mode change in the 15–20 ns range from the π-mode to a fivefold magnetron mode, which becomes the TE_{31} mode at the output (also reported and explained in [2]).

As in [2], at high magnetic fields close to the Buneman–Hartree limit, the output microwave power develops relatively low-frequency modulations, while the RM operates in the π-mode. This feature was demonstrated numerically and explained by an analytical model.[3] It was shown that these modulations are the result of the electron space charge accumulation in the potential well, formed within the upstream reflector–anode–downstream reflector volume. As electron emission develops, excess charge can form within the magnetron volume, which is released by either reduction of emission by the excess space charge, but also as an axial electron current flowing toward the two reflectors, which reflect this charge back to the magnetron. When sufficient charge is released, emission strengthens until charge returns to the RM. This nonlinear dynamic process becomes periodic,

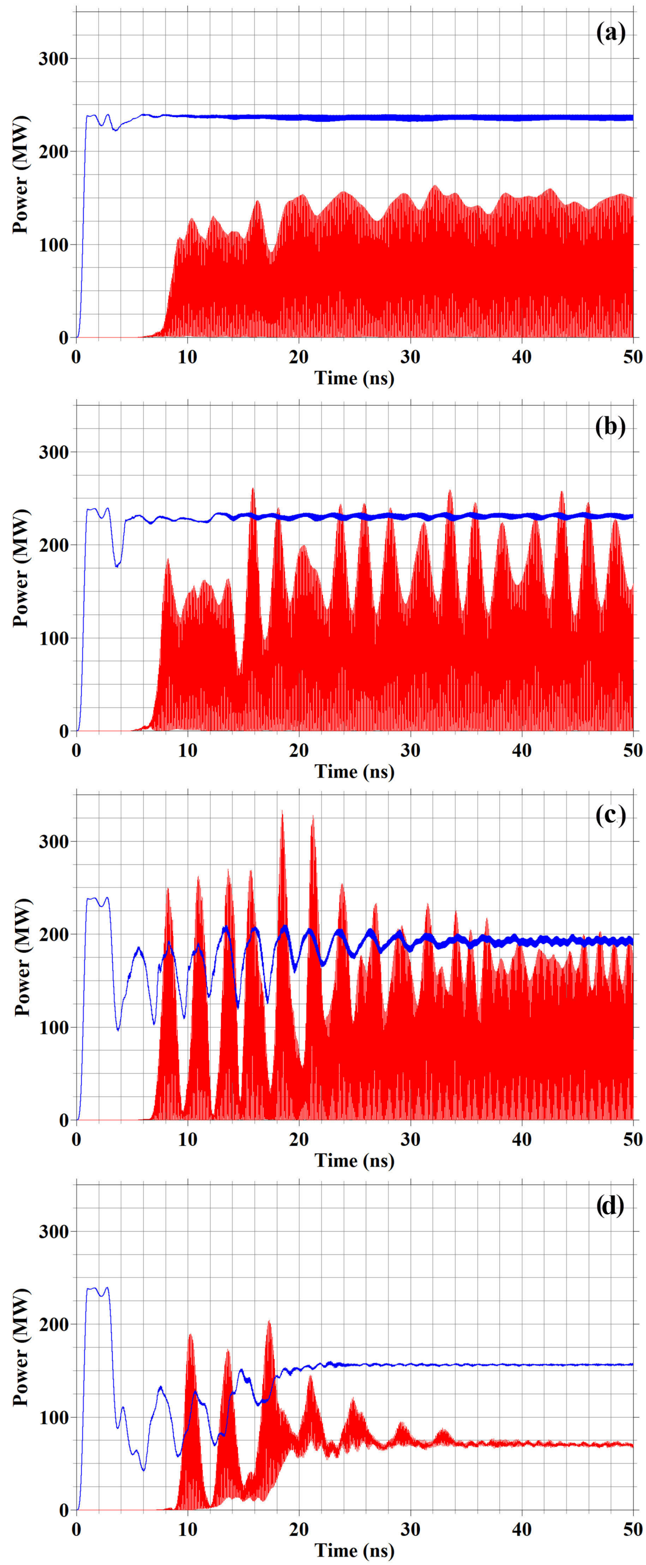

Fig. 2. Time dependence of the input (blue) and output (red) power for the simulated MDO (Fig. 1) for an applied voltage of 170 kV rising in 1 ns and an axial magnetic field of (a) 0.4, (b) 0.45, (c) 0.55, and (d) 0.6 T.

with a period equal to the axial travel time of the charge toward and back from the reflectors. This travel time determines the low-frequency modulation observed in the generated microwaves. When maximum charge is contained in the magnetron, limited by the magnetic field and energy conservation, a maximum microwave power can be obtained up to a time-averaged power of 50%. This process, though, is highly nonlinear and can become unstable.

III. Experimental Set-Up and Diagnostics

Experiments using the MDO of Fig. 1 were carried out using a linear induction accelerator (LIA) as its input power generator.[3] The LIA produces voltage and current amplitudes of ~400 kV and ~3.5 kA, respectively, with a ~50 ns rise time, and ~150 ns full-width-at-half-maximum (FWHM) pulse when operating with a matched load and at a maximal charging voltage of 2.6 kV of the primary energy storage capacitor. External views of the magnetron connected to the MDO are shown in Fig. 3, together with a general sketch of the experimental setup and the axial distribution of the external magnetic field. As in [3], the RM anode was machined from aluminum, and the dimensions of both the RM and the DOA are the same as those simulated in Section II.

The cathode emitter contained six 0.5-mm grooves, and it had a diameter of 7 mm, the same as that which gave the best performance in [3]. The supporting rods had the same diameter as the emitter and were hard anodized to avoid breakdown. The upstream 30-mm diameter reflector was located at a distance of 40 mm from the anode, and the downstream reflector was tested with diameters of 10, 20, and 26 mm and at distances of Z = −10, 0, 10, 20, 30 mm relative to the end of the DOA. Z = 0 is pointed out in Fig. 3(a). The MDO and the waveguide were located inside a 105-mm diameter stainless steel tube [see Fig. 3(a)]. Vacuum at a level of 5×10^{-3} Pa was maintained by a turbomolecular pump.

A solenoid was wound on the outer tube [3], producing an external axial magnetic field pulse of amplitudes up to 1 T and a half period of 15 ms along a length of 30 cm, where the MDO and the reflectors were located. The axial magnetic field distribution is shown in Fig. 3(a). The long-duration magnetic field pulse was necessary to allow for magnetic field diffusion through the stainless steel and aluminum anode parts. The long waveguide (60 cm), see Fig. 3(a), prevented electrons from reaching the Perspex output window in case of overflow above the downstream reflector. In addition, permanent magnets were placed along the tube to deflect remnant electrons [see Fig. 3(b)]. These measures were sufficient to avoid breakdown and plasma formation along the surface of the output window.

The voltage and total current waveforms were measured using a capacitive voltage divider (VD) and a self-integrating Rogowski coil (RC). The microwave electric field was measured as described in detail in [3]. We used the same D-dot sensor (model SFE-10G, Montena)[8] located in the far-field (120 cm from the output window). The D-dot sensor was calibrated in the 9.0–10 GHz frequency range as described in [3], and the uncertainty of this calibration was ±0.5 dB. The voltage of the microwave signal was registered by a Tektronix oscilloscope DSA 73304-D, 33 GHz, 100 GS/s

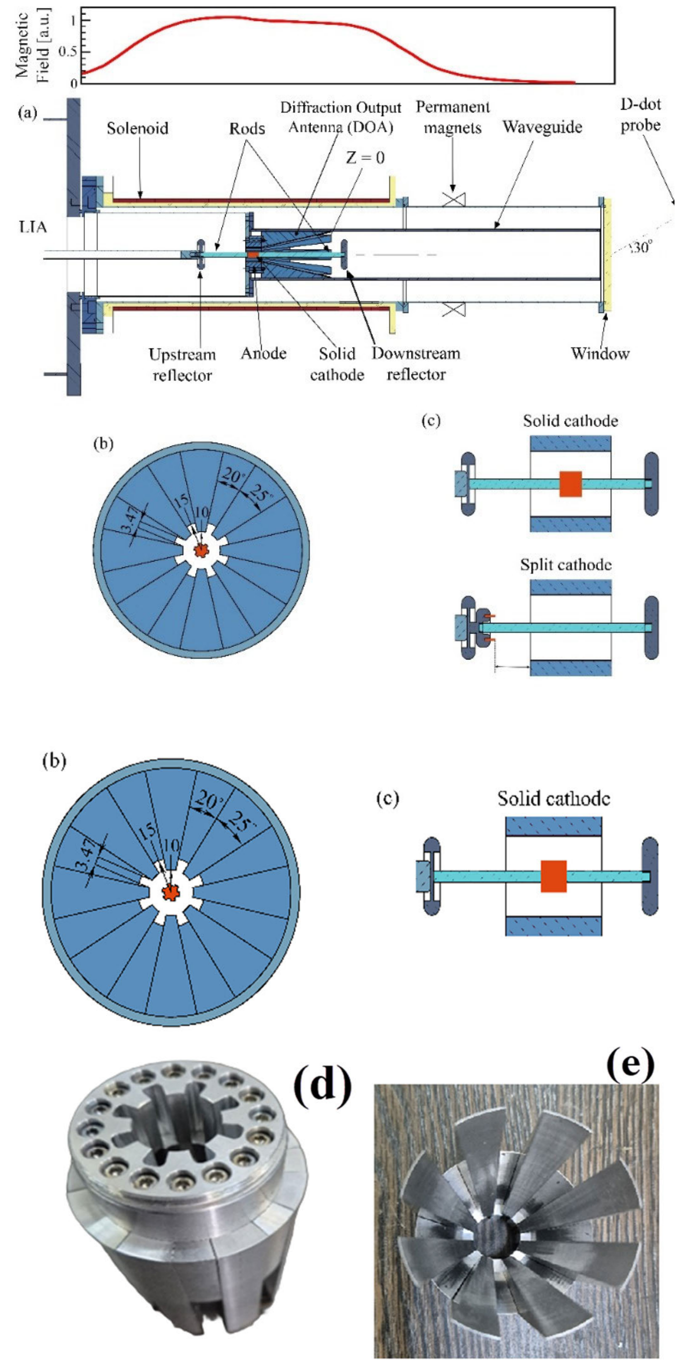

Fig. 3. (a) Experimental setup overlayed with the distribution of the axial magnetic field. (b) Dimensions of the magnetron and the DOA. (c) Pictures of the RM anode block. (d) Frontal view of the DOA.

using the same frequency-calibrated cable and attenuators. The spatial distribution of the microwave electric field measured at a distance of 120 cm from the output window along two polarization directions of the D-dot sensor (vertical and horizontal) in the horizontal plane with azimuthal intervals of 5° was found similar to that obtained in [3]. However, in the present experiments, the amplitudes of the measured electric fields in the vertical polarization E_v were found to be ~1.45 times higher than in the horizontal polarization,

E_h, in contrast to [3], where these were the same. The total electric field was determined as $E = (E_v^2 + E_h^2)^{0.5}$, and the power flux density at each polar angle was estimated as $P[\mathrm{W/cm^2}] = [E(\mathrm{V/cm})]^2/361$.[9] Using spatial electric field distribution and assuming its azimuthal uniformity, i.e., that the radiation pattern is rotationally symmetric, the total instantaneous microwave power and the electronic efficiency of the HPM generation, $\eta = (P_{\mathrm{MW}}//P_{\mathrm{gen}}) \times 100\%$, were calculated, where P_{gen} is the product of the voltage and current at a time corresponding to the HPM's maximum power (P_{MW}).

IV. Experimental Results

We varied the magnetic field amplitude, the diameter, and the location of the downstream reflector relative to the downstream end of the DOA for the same 2.4 kV LIA charging voltage. Negligibly small microwave power is generated for either 10- or 20-mm diameter downstream reflectors placed at a distance Z = −10 cm inside the DOA or at the end of the DOA, Z = 0. When this reflector was located downstream from the DO, the power of the HPM increased drastically and reached its maximum, for the 20-mm diameter reflector, when placed at Z = 10 mm. All other experiments were carried out for this configuration. At present, we have no precise explanation of such strong dependence on the position of the downstream reflector. We assume that the position of the reflector influences the dynamics of electron space change oscillations in the potential well formed between the reflectors. Also, it is possible that when the reflector is placed inside the DO, it interferes with its operation. In the absence of the downstream cathode rod extension and reflector, that is, a conventional MDO configuration, the output microwave power was ≤ 30 MW, corresponding to an instantaneous electronic efficiency of ≤ 30%.

As for the larger MDO,[3] microwave generation started only at $B_z > 0.4$ T, but the maximum microwave power was <10 MW with a pulse duration of ~60 ns. Increasing the magnetic field leads to increasing power and decreasing pulse duration. Maximum power was obtained in the magnetic field range of 0.6–0.75 T. In the simulations of Section II, maximum power is reached at a lower magnetic field, and it continues as long as the voltage is on. In Fig. 4, we present the results at $B_z = 0.7$ T. One can see a short-duration (~20 ns) HPM pulse with peak power reaching ~120 MW [Fig. 2(b)] with a frequency of ~9.5 GHz [Fig. 4(c)]. The peak power of the HPM pulse was in the range of 110 ± 10 MW in a series of 6 shots. The envelope of the microwave power reaches the value of the total input power, indicating that the electronic efficiency can reach 100%. The envelope consists of a few modulations of period ~2 ns compared to ~1.5 ns in Fig. 2(b), which is consistent, in particular, since Z = 1 cm in simulations compared to 2 cm in the experiments.

Let us note in Fig. 4(a) that the small amplitude of the current, <130 A, during the first ~70 ns of the voltage pulse is followed by a ns-timescale increase in the current up to ~1 kA. The latter is accompanied by the generation of an HPM pulse and a fast decrease in the voltage from ~320 to ~180 kV due to the LIA's finite impedance. The initial 70-ns small amplitude current indicates the accumulation of

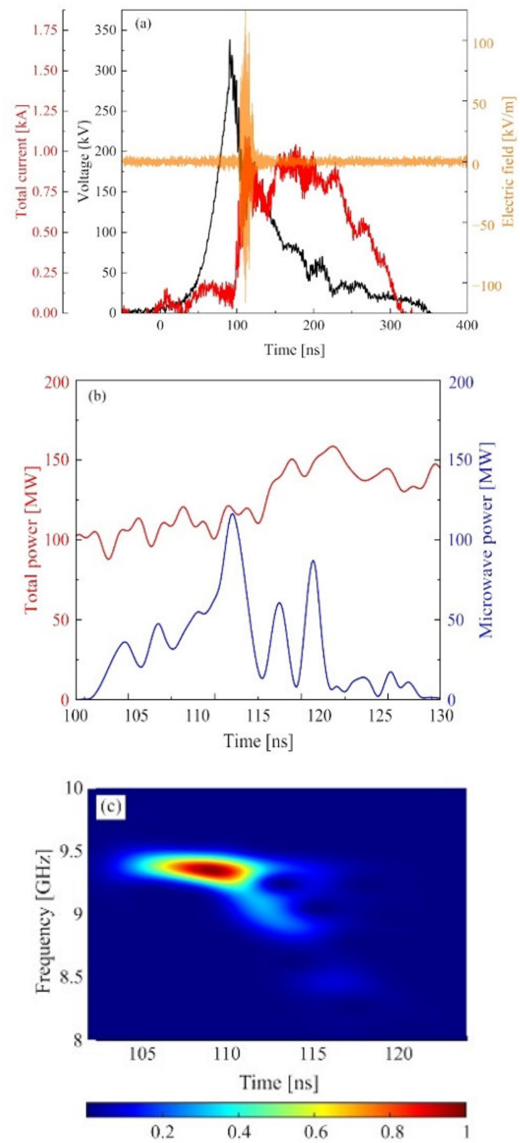

Fig. 4. (a) Waveforms of the voltage, current, and microwave electric field. (b) Total input power and the envelope of the microwave power. (c) FFT of the microwave pulse. $B = 0.7$ T.

the space charge in the potential well formed between the reflectors before it expands sufficiently toward the anode, resulting finally in high efficiency microwave generation.

The very short duration of the HPM pulse in Fig. 4 cannot be related to cathode explosive emission plasma expansion because pulse shortening occurs earlier than possible plasma expansion in the relatively large axial magnetic field. The decrease in voltage can also lead to a decrease in microwave power, but not necessarily to the termination of microwave generation. We also considered the extremely high azimuthal electric fields developing along the line connecting the edges of each cavity, which, according to the simulations, reaches ~700 kV/cm, and can lead to explosive emission plasma[10] from the vane edges. Because of the very small cavity gap (3.47 mm), propagation of plasma ~0.5 mm from both sides with a critical density of $> 2 \times 10^{12}$ cm^{-3} can significantly

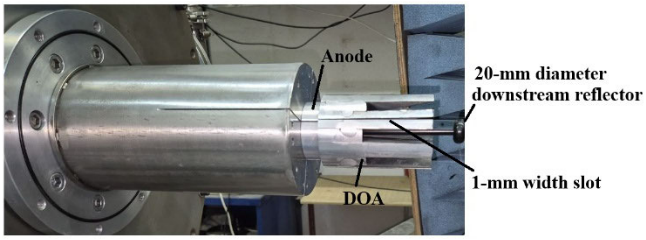

Fig. 5. External view of the RM with DOA and 1-mm wide slits. The outer tube and the magnetic coil are not present in this picture.

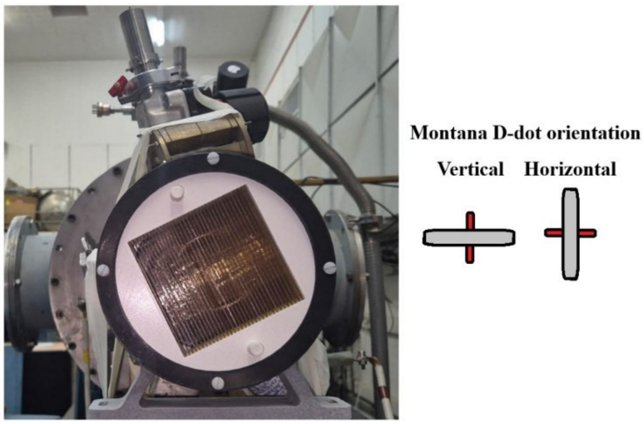

Fig. 6. External view of the QWP placed at the output of the Perspex window. The dipoles of the D-dot are shown in red color.

change the resonant properties of the cavities, possibly leading to termination of microwave generation. To avoid this effect, we hard-coated the anode block with 80-μm thick aluminum oxide, but this had no effect on the short duration of the generated HPM pulses. Visible inspection of the anode after ~10 shots showed damage on the vane surface coating. It is possible, though, that anode breakdown plasma formation is here the principal cause for HPM pulse shortening in X-band RMs, which cannot be solved by introducing a split cathode.[11]

We also tested the above magnetron in a segmented configuration.[12] Namely, we made four longitudinal 1-mm wide slits in four nonadjacent anode vanes, the DOA, and the waveguide, dividing the system into four segments to allow almost simultaneous external magnetic field penetration through the gaps between the segments (see Fig. 5).

Without the slits, we usually used a magnetic field rising over a time of ~6 ms, sufficient for magnetic field diffusion through the magnetron structure. However, this requires a power supply with stored energy of ~2.5 kJ to produce a magnetic field of ~0.7 T. This is ~8.7 times larger than the energy stored in the primary capacitor (100 μF, charging voltage of 2.4 kV) of the LIA. Experiments carried out with this segmented MDO produced almost exactly the same HPM pulse obtained with the ordinary MDO. Thus, as for the S-band RM [12], where these slits were tested for the first time and magnetic fields with a duration of ~80 μs were sufficient to produce the same microwave fields, we showed here that the same approach can be applied for an X-band magnetron. This allows one to use a primary supply of only ~300 J total stored energy sufficient to produce magnetic fields of ~0.7 T in the system with a total length of 60 and 6 cm in diameter. Experiments carried out with this segmented MDO produced almost the same microwave power and frequency as obtained without slits.

TABLE I

Measurements of the Electric Field's Horizontal and Vertical Components With and Without QWP

Orientation of D-dot dipoles	Without QWP	With QWP
Vertical	58 ±1 kV/m	59 ±1 kV/m
Horizontal	40 ±1.5 kV/m	67 ±2 kV/m

Additionally, in these experiments, we determined the polarization state of the output electromagnetic wave by manipulating it using a high-efficiency dielectric meta-surface waveplate. We designed and tested a quarter-wave plate (QWP) composed of a 1-D grating of alternating 1-mm thick Ultem plates with 2-mm air gaps in between. The QWP parameters were calculated using a modified effective medium theory and optimized using finite-element frequency-domain (FEFD) simulations. The QWP was placed between two rotating antennas, and the transmission and reflection were measured along orthogonal axes. The QWP was found to have high, ~85%, transmission efficiency and low mode distortion in the frequency range of 9–11 GHz. The retardation was found to be 90° ± 3° in the frequency range of 8.4–9.7 GHz, resulting in a conversion efficiency above 90% for the entire bandwidth and allowing for efficient conversion of circular to linear polarization.

In the MDO experiments, the QWP was placed on the output Perspex window, as seen in Fig. 5. Four sets of experiments, each of 5 shots, were carried out at B_z = 0.65 T with and without the QWP, when the orientation of the dipoles of the D-dot sensor was either vertical or horizontal.

In Table I, one can see the results of these measurements showing that without the QWP, the horizontally polarized electric field is ~1.45 times smaller than the electric field with vertical polarization. This is an indication of the high-order mode of the MDO output. We cannot directly measure the phase difference between the vertically and horizontally polarized electric field components. However, the application of the QWP changes the amplitude of the horizontal component, which can be the result of an elliptically polarized output wave. That is, an increase in the amplitude of the horizontal component 1.6 times in the presence of the QWP indicates that the initial phase difference between the components was close to 90°. Thus, this type of QWP can be efficiently used for polarization manipulation and for characterizing HPM pulses of powers exceeding 100 MW and duration of ≤ 20 ns.

V. Summary

We presented the results of numerical and experimental studies of a more compact X-band relativistic MDO supplied by voltage pulses of ≤350 kV and ≤150 ns duration, with a DOA less than half the output radius and length of the

MDO reported in [3]. It was shown that this MDO generates X-band HPM pulses with power exceeding 100 MW and a pulse duration of ≤20 ns and electronic efficiency reaching 100%. We also showed that this MDO operates successfully when it is composed of four segments separated by gaps to allow the external magnetic field to penetrate almost simultaneously. This decrease in the MDO diameter and length and the segmentation make this device not only compact but also reduce the energy requirements of the magnetic field power supply drastically, making it possible to operate with this device repeatedly. The main disadvantage of the present compact X-band MDO is pulse shortening. We are looking for ways to eliminate this problem by feeding the MDO with a split cathode and widening the anode cavity gaps. We also presented a novel QWP design that operates without breakdown at HPM power exceeding 100 MW.

REFERENCES

[1] J. Benford, "History and future of high power microwaves," *IEEE Trans. Plasma Sci.*, vol. 52, no. 4, pp. 1137–1144, Apr. 2024, doi: 10.1109/TPS.2024.3391732.

[2] J. G. Leopold et al., "An optimized design for an X-band high power relativistic diffraction output A8 magnetron," *Phys. Plasmas*, vol. 32, no. 8, Aug. 2025, Art. no. 083102, doi: 10.1063/5.0281707.

[3] O. Belozerov et al., "A novel high-power X-band relativistic diffraction output magnetron," *IEEE Trans. Plasma Sci.*, vol. 53, no. 11, pp. 3285–3292, Nov. 2025, doi: 10.1109/TPS.2025.3612305.

[4] J. G. Leopold et al., "A novel A10 relativistic diffraction output high-power magnetron operating at 9.8 GHz," *IEEE Trans. Plasma Sci.*, vol. 53, no. 11, pp. 3308–3312, Nov. 2025, doi: 10.1109/TPS.2025.3615228.

[5] N. F. Kovalev, B. D. Kolchugin, V. E. Nechaev, M. M. Ofitserov, E. I. Soluianov, and M. Fuks, "Relativistic magnetron with diffraction coupling," *Sov. Tech. Phys. Lett.*, vol. 3, pp. 430–433, Oct. 1977.

[6] O. Belozerov et al., "Experimental research on an X-band magnetron fed by solid and split cathodes," *IEEE Trans. Plasma Sci.*, vol. 52, no. 7, pp. 2749–2759, Jul. 2024, doi: 10.1109/TPS.2024.3450928.

[7] B. Goplen, L. Ludeking, D. Smith, and G. Warren, "User-configurable MAGIC for electromagnetic PIC calculations," *Comput. Phys. Commun.*, vol. 87, nos. 1–2, pp. 54–86, May 1995, doi: 10.1016/0010-4655(95)00010-d.

[8] *Montena Technology*. Accessed: Aug. 13, 2024. [Online]. Available: https://www.montena.com

[9] Y. P. Raizer, *Gas Discharge Physics*. Berlin, Germany: Springer-Verlag, 1991.

[10] G. A. Mesyats and D. I. Proskurovsky, *Pulsed Electrical Discharge in Vacuum*. Berlin, Germany: Springer-Verlag, 1989.

[11] J. G. Leopold et al., "Experimental and numerical study of a split cathode fed relativistic magnetron," *J. Appl. Phys.*, vol. 130, Jun. 2021, Art. no. 034501, doi: 10.1063/5.0055118.

[12] O. Belozerov et al., "Characterizing the high-power-microwaves radiated by an axial output compact S-band A6 segmented magnetron fed by a split cathode and powered by a linear induction accelerator," *J. Appl. Phys.*, vol. 133, no. 13, Apr. 2023, Art. no. 133301, doi: 10.1063/5.0138769.